Journal of Materials Chemistry C

Accepted Manuscript

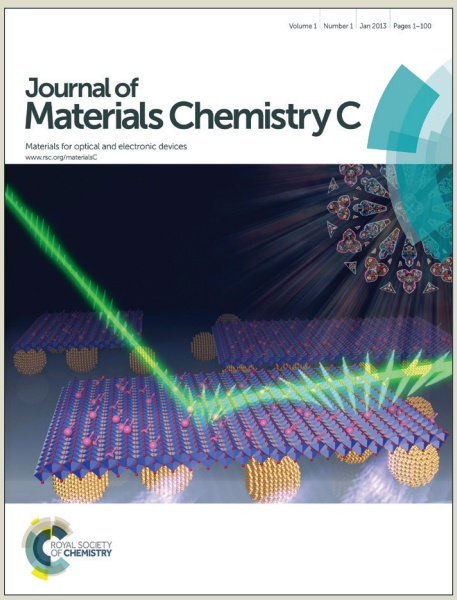

ROYAL SOCIETY OF CHEMISTRY

www.rsc.org/materialsC

Journal Name Journal of Materials Chemistry C Dynamic Article Links►

Cite this: DOI: 10.1039/c0xx00000x

www.rsc.org/xxxxxx

ARTICLE TYPE

Fabrication of Nitrogen-Doped Graphene Quantum Dot from MOFs-Derived Porous Carbon and its Application for Highly Selective Fluorescent Detection of Fe^{3+}

Hongbo Xu,[ab] Shenghai Zhou,[a] Lili Xiao,[ab] Huanhuan Wang,[a] Shouzhu Li[a] and Qunhui Yuan*[a]

Received (in XXX, XXX) XthXXXXXXXXX 20XX, Accepted Xth XXXXXXXXX 20XX
DOI: 10.1039/b000000x

Nitrogen doping of carbon quantum dot results in improved fluorescence performance and a wider range of applications in photocatalysis, sensor and bioimaging, *etc*. Herein, a water-soluble and well-crystallized nitrogen-doped graphene quantum dot (N-GQD) has been obtained by using a MOF-derived carbon (ZIF-8C) as a new source of graphitic sheets. The preparation is based on a rapid, eco-friendly and efficient acid vapour cutting strategy, which is different from previously reported solution chemistry routes. The as-prepared N-GQD is photoluminescent and exhibits an excitation-independent behaviour. Because of the presence of O-functional groups on the surface, the obtained N-GQD can serve as a fluorescent sensing probe for highly selective detection of Fe^{3+} ions with a detection limit of 0.08 μM (at a signal-to-noise ratio of 3). This work would enable new opportunity for the wider use of MOFs-based material and also contributes to the fluorescent analysis of Fe^{3+}.

Introduction

As a novel luminescent carbon material, graphene quantum dot (GQD) has attracted growing interest because of its strong photoluminescence, low toxicity and good solubility.[1] These unique properties make GQDs suitable for a wide variety of promising applications in optoelectronic devices,[2] photocatalysis,[3] sensing,[4] and bioimaging.[5] Recent research has shown that the introduction of nitrogen to the nanometer-sized carbon materials can drastically alter their electronic characteristics and thus expand their range of applications.[6] For example, Li *et al*. found that the properties of GQDs could be drastically tuned by nitrogen-doping. The various nitrogen-doped colloidal graphene quantum dots (N-GQDs) obtained by solution chemistry approach in their study exhibited a size-dependent electrocatalytic activity for the oxygen reduction reaction.[7] Gong *et al*. reported an efficient two-photon fluorescent N-GQD probe with low cytotoxicity and good photostability for cellular imaging.[8] They demonstrated that the nitrogen-doping onto GQD with strong electron-donating dimethylamido groups resulted in a red shift of its fluorescence emission. The large π-conjugated graphene sheets and the strong electron donating effect of dimethylamido facilitated the charge transfer efficiency and led to strong two-photon-induced fluorescence for N-GQD. Jiang *et al.* proved that N-GQD could be used as an efficient photocatalyst for photochemical synthesis of silver nanoparticle loaded porous graphitic C_3N_4 (Ag/p-g-C_3N_4).[9] The successful and efficient preparation of Ag/p-g-C_3N_4 composite was ascribed to the excellent electron-donating capability of photo-excited N-GQD, which acts as both photosensitizer and reducing agent because of its broad visible light absorption under visible light. Generally, the preparation approaches of the N-GQDs can be summarized as electrochemical synthesis,[10] organic synthesis,[7] hydrothermal synthesis,[11] solvothermal preparation[8] and acidic oxidation.[12,13] Since the experimental attempt for the fabrication of N-GQDs is only a recent effort, the obtaining of the N-GQDs with good chemical and physical properties in a way of mass production or through cost and time effective methods has yet to be reached.[14] Therefore, it is highly desirable to explore facile and eco-friendly routes for the large-scale preparation of untainted N-GQDs with good solubility.

Herein, we present an acid vapour cutting method for the rapid obtaining of N-GQDs by simply cutting a metal-organic framework (MOF) derived porous carbon with incorporated nitrogen atoms. Recently, one of the most rapidly growing applications of MOFs was being used as precursors for the preparation of ordered porous carbons, due to their porous crystalline structures that consist of metal ions and organic ligands.[15] Based on the compositive diversity of MOFs, heteroatom doped porous carbons can also be obtained using MOFs constructed from heteroatom containing organic ligands.[16] More interestingly, the MOF-derived carbons would contain graphitic sp^2 hybridized structures under suitable treatments.[17] For instance, by the calcination of a parent Al-based MOF, Yamauchi *et al.* prepared a fibrous nanoporous carbon with a superior sensing capability toward toxic aromatic substances. Such superior sensing capability for toluene vapour was ascribed to the higher affinity of the graphitic carbon containing sp^2-

hybridized carbons for aromatic hydrocarbons.[18] From a practical point of view, the graphitic structures of the MOFs-derived carbons may possibly be used to obtain nanometer-sized graphene sheets with confined shapes since the synthesis of GQDs can readily be achieved from starting materials with small domains of sp^2 hybridized carbons, as pointed out by Zhu *et al.* and Pan *et al.*[19, 20]

Lately we have demonstrated that the carbonization of ZIF-8 (a MOF material) led to nitrogen-rich porous carbon nanopolyhedron (ZIF-8C) for the fabrication of chemically modified electrode, and its application in Pb(II) and Cd(II) detection with an electrochemical method.[21] This MOF-derived carbon possesses high specific area, high percentage of nitrogen doping, graphitic sp^2 hybridized structures and high-yield during the preparation. Based on this work, we developed a facile preparation of fluorescent N-GQD by acid vapour cutting of this MOF-derived carbon. This acid vapour cutting method has previously been used for the purification and functionalization of carbon nanotubes.[22] Compared with carbon nanotubes, the larger surface area and the more porous structures of the nitrogen-rich ZIF-8C provide more cutting points for the acid vapour to react with, leading to a rapid (less than 5 h) and high-yield (*ca.* 38%) synthesis of the N-GQDs. This approach may provide a way to avoid time-consuming syntheses and special organic precursors for fabrication of the GQDs,[1] due to a high-yield preparation of MOFs and nitrogen-rich MOFs-derived carbons.

As an application example, the obtained N-GQD was used as a sensing probe for the selective detection of ferric ions in comparison with other metal ions (Ag^+, Al^{3+}, Ca^{2+}, Zn^{2+}, Cd^{2+}, Co^{2+}, Cu^{2+}, Fe^{2+}, Hg^{2+}, K^+, Mg^{2+}, Mn^{2+}, Ni^{2+}, Pb^{2+} and Na^+) in aqueous solution. Fe^{3+} can quench the photoluminescence (PL) of the N-GQDs because it facilitates charge transfer processes by forming the Fe-N-GQD complex.[23] This allows the N-GQD to be used as a fluorescent probe for Fe^{3+} with a detection limit of 0.08 μM (at a signal-to-noise ratio of 3). And also, based on the diversity of the structural organic ligands of MOFs, S-GQDs or N, S-GQDs can also be obtained by using MOFs-derived porous carbon containing S or N, S as raw materials. Therefore, the presented method allows for a new application of MOFs-based materials and also will expand the scope of heteroatom doped GQDs.

Experimental

Reagents and Apparatus

All chemicals were of analytical grade and used without further purification. X-ray powder diffraction (XRD) data were collected on a Siemens D5005 diffractometer (Siemens, Germany). Nitrogen adsorption-desorption experiments were performed on a N_2 adsorption apparatus (Quantachrome Insturments, USA). X-ray photoelectron spectroscopy (XPS) experiments were performed using an Al Kα source, with energy of 1486.6 eV at room temperature. Transmission electron microscopy (TEM) images were recorded on a JEM-3010 (Japan). Atomic force microscopy (AFM) was performed on a Multimode 8 (Bruker, USA). The UV-vis spectra were recorded on a Shimadzu UV-1800 spectrometer (Shimadzu, Japan). The fluorescence intensity of the N-GQDs solutions (pH≈3) were measured on an F-7000 luminescence spectrometer with an excitation slit width of 10 nm.

Synthesis of ZIF-8 nanocrystals and ZIF-8 derived carbon (ZIF-8C)

ZIF-8 was synthesized according to previously reported work.[17, 21] The detailed procedures followed were: 0.395 g of 2-methylimidazole and 0.387 g of Zn $(NO_3)_2$ $6H_2O$ were dissolved in 30 ml methanol separately to generate two solutions. These two solutions were mixed and aged for 24 h at room temperature. The white ZIF-8 crystals were retrieved by washing with methanol. The obtained white powder was pre-heated at 150 ℃ for 3 h under a nitrogen flow and then heated at 300 ℃ for an additional 2 h at a heating rate of 2 ℃/min. The temperature was finally increased to 800 ℃ and maintained there for 4 h, leading to the formation of ZIF-8C black powder. After carbonization, the HCl (35 wt. %) was used to remove the zinc residue.

Preparation of the N-GQDs

A fast preparation of the N-GQDs was achieved with a steaming procedure. Scheme 1 illustrates the synthesis route of the N-GQDs. Briefly, by using a ZIF-8C that derived from a ZIF-8 nanocrystal as raw material, the N-GQDs was obtained at relatively low temperature via an acid vapour cutting strategy. The details of this approach were as follows: 0.25 g ZIF-8C powder was loaded on the porous SiO_2 griddle of a glass steamer (Scheme 1). The glass steamer was then placed into an autoclave containing 2 ml concentrated HNO_3. This autoclave was then moved to an oven for steaming treatment at 160 ℃ for 5 h. The steamer in the autoclave was subsequently transferred to a clean beaker and washed with ultrapure water using in-situ filtration (Scheme 1). Finally, a yellow filtrate was collected and labelled as N-GQDs solution.

With this steaming strategy, the N-GQDs can be conveniently separated by using a self-designed glass steamer with an embedded porous SiO_2 griddle, on which the unreacted residue was retained. Therefore, contamination from the experimental additives or unreacted residues of the as-prepared N-GQDs can be avoided compared with the solution routes. Compared with the previous acidic oxidation method,[13] the vapour cutting approach only required about 10% HNO_3 for the preparation of N-GQDs of the same amount. This makes the current vapour cutting method relatively easy and eco-friendly. Furthermore, the cutting occurred in an acid vapour medium allows the hydrophilic functional groups to be retained on the surface of the N-GQD material, thus makes the N-GQD material water-soluble.

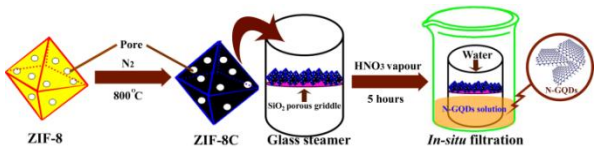

Scheme 1. Schematic diagram of the preparation of the N-GQDs.

Results and Discussion

Structural Characterization of ZIF-8, ZIF-8C and N-GQD

The obtaining of pure ZIF-8 with a cubic $I\bar{4}3m$ group was proved by the diffraction peaks of the ZIF-8 nanocrystals in the XRD spectrum, which were identical to those reported by Torad *et al.*[17] (shown in Figure S1).

The porous structures of the ZIF-8 and ZIF-8C with typical type-I isotherm features were evaluated by nitrogen adsorption-desorption analysis (shown in Figure S2). The specific surface areas were estimated to be 949 m^2/g for ZIF-8C and 1302 m^2/g for ZIF-8. The highly resolved TEM images (see in Figure S3) with similar features to the previously reported results also proved the existence of abundant pores in ZIF-8 and ZIF-8C.[17] These results indicated the retaining of big amount of open pores in ZIF-8C.

After the carbonization, white powered ZIF-8 turned to black powder with the main structure of ZIF-8 being retained, as shown in the photo and the scanning electron microscopy (SEM) images in Figure 1. The nitrogen content in ZIF-8C was estimated to be *ca.* 25% upon the SEM/EDS measurement, indicating that nitrogen-rich MOFs-derived porous carbon was successfully obtained.

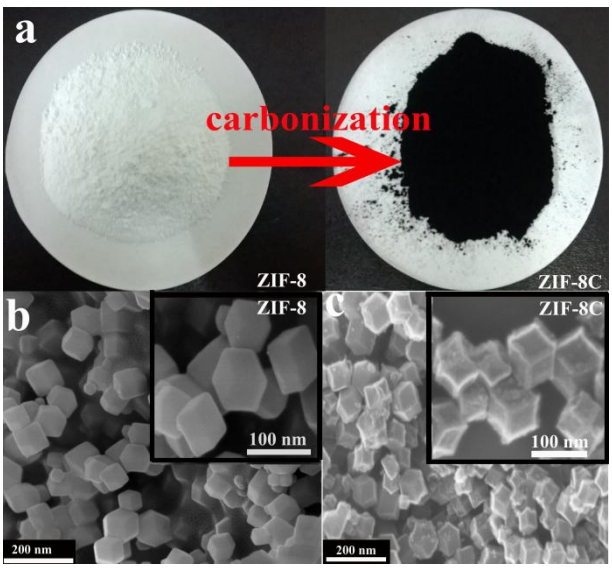

Figure 1. (a) Contrastive photographs of ZIF-8 powder before and after carbonization. SEM images of ZIF-8 nanocrystals (b) and ZIF-8C powder (c).

A typical transmission electron microscopy (TEM) image of the ZIF-8C-derived GQDs was shown in Figure 2a. The N-GQD exhibited a relatively narrow size distribution in a range of 1.3-2.7 nm with an average diameter of 2 nm based on the statistical analysis of about 100 dots (see inset in the bottom of Figure 2a).The high resolution TEM (HRTEM) image indicated that the N-GQD (up inset of Figure 2a) was highly crystalline, similar to previously reported N-GQD materials.[14] The lattice fringes with a spacing of 0.214 nm agrees well with the (100) facet of graphene and the previous reported N-GQD by Liu Q. *et al.*[24] The thickness of the N-GQDs was further characterized by atomic force microscopy (AFM) after the deposition of the N-GQDs onto a freshly exfoliated mica (Figure 2b). The typical topographic height less than 1.2 nm (Figure 2c) suggested that the N-GQDs generally contained 1-2 layers of graphene sheets.[25] This result proved that the ZIF-8C contained many small domains of graphene sheets which could be used for the preparation of N-GQD materials. It was also observed that the ZIF-8C transformed into a sphere-like particle with a smaller size after acid vapour cutting (Figure S4), indicating an etching of the porous carbon nanoparticles and the formation of the N-GQDs material.

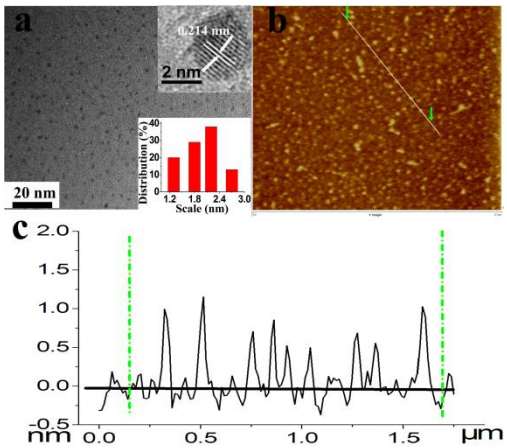

Figure 2. (a) A typical TEM image of the N-GQDs. The upper and lower inset represents the graphitic layers of one GQD under HRTEM and the size distribution of the N-GQDs, respectively. (b, c) AFM image and its corresponding height profile of the N-GQDs.

Figure 3a shows a Fourier-transform infrared (FT-IR) spectrum with distinguishable features of C-N groups at 1038 cm^{-1}, which confirms the successful preparation of the N-GQD material.[26] The as-prepared N-GQD was found to be O-rich material with FT-IR peaks at *ca.* 3401cm^{-1} (ν_{OH}), 1638 cm^{-1} ($\nu_{C=O}$), 1383 cm^{-1} (ν_{C-OH}) and 1097 cm^{-1} (ν_{C-O}) from hydroxyl and carbonyl groups, respectively.[26]

X-ray photoelectron spectroscopy (XPS) was also carried out to determine the surface contents and chemical configurations of the N-GQD materials. The XPS spectrum in Figure 3b showed a predominant graphitic C 1s peak at about 284 eV, a N 1s peak at about 401 eV and an O 1s peak at about 532 eV.[10, 26] The six deconvoluted peaks in the C 1s spectrum in Figure 3c could be assigned to O-C=O (289.2 eV), C=O (288.5 eV), C-O (286.3 eV), C-N (285.3 eV), C-C (284.8 eV) and C=C (284.3 eV) from left to right.[26] This assignment agrees well with the conclusion deduced from the FT-IR spectrum. The estimated nitrogen content (*ca.* 4.9%) was close to the previously reported value, confirming the successful doping of nitrogen into graphene quantum dots.[10] Figure 3d also showed a high resolution N 1s spectrum of the N-GQD, which revealed the presence of several nitrogen functional groups: pyrrolic-N (N1, binding energy (BE) = 400.3 ± 0.2 eV), quaternary nitrogen (N2, BE = 401.2 ± 0.2 eV) and the N-oxides of pyridinic-N (N3, BE = 402.8 ± 0.4 eV).[27] The high oxygen content of *ca.* 37% led to the high solubility of the N-GQD in aqueous solution. The oxygen groups on the surface of the N-GQD, such as the hydroxyl and carbonyl groups, will also result

in a strong affinity toward metal ions.[23] These characterizations will benefit the application of this N-GQD material in aqueous solution, such as metallic ions sensing, as will be discussed latter in this manuscript.

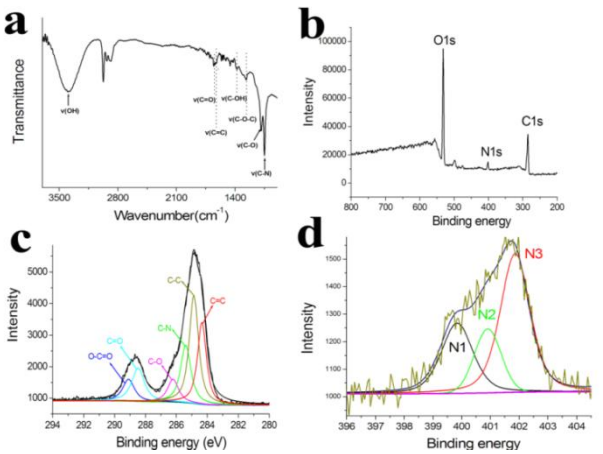

Figure 3.(a) FT-IR spectrum of the N-GQDs. (b) XPS spectrum of the N-GQDs. (c, d) High-resolution XPS C1s and N1s spectra of the N-GQDs.

The synthesized N-GQD was further characterized by XRD and Raman spectroscopy. The XRD pattern in Figure 4a contained a broad peak centered at 22.6 º, corresponding to a (002) interlayer spacing of the N-GQDs. Such low diffraction degree suggests a large interlayer spacing (0.393 nm), which may be due to the high oxygen content of this N-GQDs, as has been pointed out by Dong *et al.*[28] In their study, the interlayer spacing of GQDs increases with the increase of oxygen content. The two Raman bands showed in Figure 4b at 1367 cm^{-1} and 1560 cm^{-1} could be attributed to the D and G bands of the carbon materials, respectively.[10] The intensity ratio of the disordered D-band to the crystallized G-band (I_D/I_G) was estimated to be *ca.* 1.26, suggesting the generation of defects and a concomitant intercalation of N atoms into the conjugated carbon backbone, which is similar to that found previously.[13]

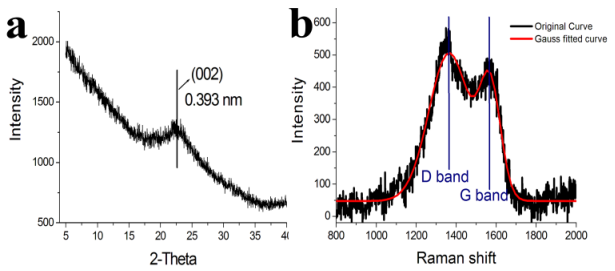

Figure 4. XRD pattern (a) and Raman spectrum (b) of the N-GQDs

UV-vis absorption and fluorescence property of the N-GQDs

The optical property of GQDs plays an important role in their applications. The UV-vis absorption spectrum of N-GQDs in water was investigated and recorded in Figure 5a. The N-GQDs give an UV-vis absorption with a peak at *ca.* 200 nm from the $\pi \rightarrow \pi^*$ transition of the aromatic sp^2 domains, as pointed out previously.[29] Compared with previous studies, in which the adsorption peak were generally found at 227 nm wavelength, this blue-shifted absorption peak at 200 nm suggests more significant oxidation on the surface of the N-GQDs, implying an increased number of hydroxyl and carboxylic groups with a strong electron drawing effect after oxidation.[8, 30, 31] Also, two wider and weaker adsorption peaks were observed at 290 and 350 nm (more clearly shown in the absorption spectra of N-GODs solution with higher concentration, in the inset of Figure 5a). These two peaks might arise from the trapping of the excited state energy of the surface states, which can lead to strong fluorescence, as suggested by Chen *et al.*[32] Accordingly, as shown in the inset in Figure 5a, the clear and yellow N-GQDs solution exhibited an intense yellow-green colour when irradiated with UV light (365nm).

The fluorescence spectra of the N-GQDs at different excitation wavelengths were obtained and shown in Figure 5b. The photoluminescence showed an excitation-independent feature, similar with GQDs reported by Zhang *et al.*[30] As shown in Figure 5b, the PL peak of the N-GQDs remained at around 490 nm when the excitation wavelength changed from 290 nm to 410 nm. This phenomenon is different from the general excitation-dependent PL emissions reported previously, in which the PL peaks shift to longer wavelengths upon an increase in the excitation wavelengths.[29,33] This excitation-independent property of the N-GQD can benefit its application by avoiding auto-fluorescence phenomenon, as pointed by Jiang *et al.*[34] The fluorescence intensity of the N-GQD changes remarkably at various excitation wavelengths from 290 nm to 410 nm with the highest fluorescence intensity obtained at 330 nm. Therefore, the excitation wavelength was selected as 330 nm for subsequent experiments.

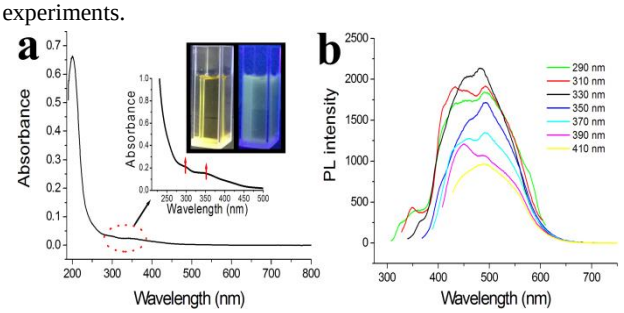

Figure 5. (a) UV-vis absorption spectrum of the N-GQDs dispersed in water. Inset: Two wider and weaker adsorption peaks at 290 and 350 nm; Photographs of the N-GQDs solutions taken under illumination of ambient light (left) and UV light (365 nm, right). (b) PL emission spectra of the N-GQDs aqueous solution at different excitation wavelengths from 290 to 410 nm.

Detection of Fe^{3+} ions

Encouraged by the strong photoluminescence and abundant surface oxygen groups of the prepared N-GODs material, we used the N-GODs for the detection of Fe^{3+} ions in aqueous solution based on the coordination between Fe^{3+} ions and phenolic hydroxyl, which has been discussed by Zhang *et al.* and Wang *et al.*[23,35] As a common element in the human body, the abnormal amount of Fe^{3+} is closely related to several diseases,

including anemia, Parkinson's disease and malaria.[36,37] Therefore, an efficient determination of Fe^{3+} is of great importance. Recently, fluorescent chemosensors with good selectivities, rapid responses and simple operations towards Fe^{3+} detection have attracted considerable attention.[36,38-41] Materials such as metal nanoclusters,[38] carbon nanodots,[39] polymer nanodots[40] and organic fluorescent molecules[41] have been used as sensing probes. These studies also show that the fabrication of label-free and interference-free Fe^{3+} sensors with high performance is still a challenge in the search of novel fluorescent sensing materials.

The fluorescence responses of the prepared N-GQDs towards different concentrations of Fe^{3+} were obtained and shown in Figure 6a. The N-GQDs solution was prepared by diluting 0.25 ml GQDs filtrate with 1.75 ml deionized water (≥18.2 MΩ). The N-GQDs content in this solution was 0.24 mg/ml based on the weight ratio of the dry products obtained by heating the yellow filtrate at 200 ℃. Certain amount of Fe^{3+} stock solution was added into the solution to reach the wanted Fe^{3+} concentrations. The fluorescence intensity at 490 nm was gradually quenched upon the increase of Fe^{3+} concentration. The fluorescence intensity had a good linear relationship with the Fe^{3+} concentration as shown in Figure 6b. The linear regression equation was defined as $I = -12.69*C_{Fe(III)} + 2170.69$ with a linear range from 1 to 70 μM ($R^2 = 0.98$). The detection limit was about 0.08 μM (at a signal-to-noise ratio of 3), which was lower than the maximum tolerance (5.4 μM) allowed by the U.S. Environmental Protection Agency in drinking water.[42] These results demonstrated that the N-GQD could be used as a promising fluorescent probe for the detection of Fe^{3+} in aqueous solution.

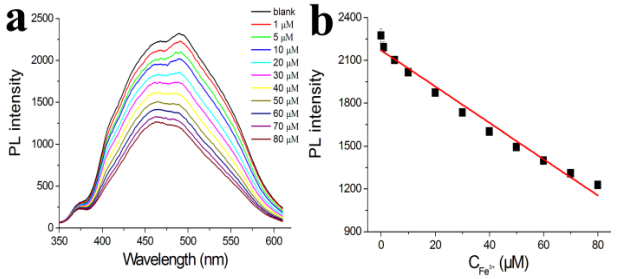

Figure 6.(a) PL emission spectra of the N-GQDs aqueous solution (0.24 mg/ml) in the presence of different concentrations of Fe^{3+} (from top to bottom: 0, 1, 5, 10, 20, 30, 40, 50, 60, 70 and 80 μM). (b) Calibration curve for Fe^{3+} detection.

To evaluate the selectivity of the proposed fluorescent probe, the effects of the potential interfering ions on the relative fluorescence intensity of the N-GQDs towards Fe^{3+} were examined at an excitation wavelength of 330 nm. Metal ions (Ag^+, Al^{3+}, Ca^{2+}, Zn^{2+}, Cd^{2+}, Co^{2+}, Cu^{2+}, Fe^{2+}, Hg^{2+}, K^+, Mg^{2+}, Mn^{2+}, Ni^{2+}, Pb^{2+} and Na^+) at the same concentration Fe^{3+} were added to the N-GQDs solution. Then the fluorescence responses were recorded. A significant lower fluorescence was observed when Fe^{3+} was added to the solution, while no obvious decrease occurred upon the addition of any other ions, as shown in Figure 7. This interference study proved that the N-GQD is highly selective for Fe^{3+} in aqueous solution.

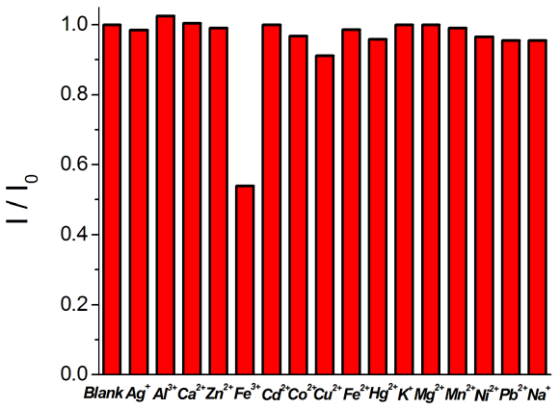

Figure 7. Normalized fluorescence intensity at λex= 330 nm of the N-GQDs aqueous solution (0.24 mg/ml) in the presence of various metal ions at the same concentration (from left to right: blank, Ag^+, Al^{3+}, Ca^{2+}, Zn^{2+}, Fe^{3+}, Cd^{2+}, Co^{2+}, Cu^{2+}, Fe^{2+}, Hg^{2+}, K^+, Mg^{2+}, Mn^{2+}, Ni^{2+}, Pb^{2+}, Na^+). I_0 and I are the PL intensities of the N-GQDs in the absence and presence of metal ions, respectively.

This high selectivity may be attributed to the specific coordination between Fe^{3+} and the phenolic hydroxyl groups as suggested in some literatures,[23, 35] based on the fact that there are abundant oxygen functional groups including phenolic hydroxyl groups on the surface of this obtained N-GQDs, as has been confirmed by the FT-IR and XPS characterization. Therefore, the Fe-N-GQDs complexes may facilitate the photo-induced charge transfer from the N-GQD to ferric ion upon its addition.[23] This photo-induced charge transfer can cause a perturbation of the electronic states of the N-GQDs as well as non-radiative transitions, thus leads to a significant fluorescence quenching.[43] For the photostability study, the obtained N-GQD was continuously irradiated under a Xe lamp (150W) for 2h. The luminescence of the N-GQDs increased by only 2.9%, indicating a good photostability of the N-GQDs (shown in Figure S5). The stability of the N-GQDs had also been checked. The N-GQDs solution maintained clear after three months storage and its PL intensity decreased only 4.5%, indicating a good long-term stability (shown in Figure S6). This good stability might benefit from the external oxygen functional groups of the N-GQDs, which ensured the good water-solubility of the GQDs and prevent the π-π aggregation among them as well.

With the calibration curve shown in Figure 6b, the application of the obtained N-GQDs for the determination of Fe^{3+} in real water sample was also investigated. In this case, the detecting N-GQDs solution was prepared using tap water instead of deionized water as diluted agent for GQDs filtrate. It is noted in Table S1 that no detectable Fe^{3+} was found in the original tap water. After the addition of a known quantity of Fe^{3+} into the detecting solutions, the measured concentrations of Fe^{3+} agreed well with the added amounts. The satisfying recovery was ranged from 98.6 % to 105.7%, indicating the developed method is feasible.

Furthermore, we compared the performance of the obtained N-GQDs with some other similar fluorescent nano-probes (Table 1). It could be seen that the present N-GQDs exhibited better or comparable performance, including wider linear range, lower detection limit and better selectivity.[38,40,44-49]

Table 1. Performance comparison of the as-prepared N-GQDs with other fluorescent nano-probes for determination of Fe^{3+}.

Fluorescent probe	Detection limit (μM)	Linear range (μM)	Response towards metal ions	Ref.
GQDs	7.22	0-80	Fe^{3+}	44
N-GQDs	0.09	1-1945	Fe^{3+}, Hg^{2+}	45
Carbon nanodots	0.32	0-20	Fe^{3+}	46
C_3N_4 nanodots	0.001	-	Fe^{3+}, Cu^{2+}	47
Polymer nanodots	-	0.1-10	Fe^{3+}	40
Au nanoclusters	3.5	5-1280	Fe^{3+}	38
Ag nanoclusters	0.12	0.5-20	Fe^{3+}	48
MOFs particles	0.9	3-200	Fe^{3+}	49
N-GQDs	0.08	1-70	Fe^{3+}	This work

Conclusions

In summary, with a MOF-derived carbon (ZIF-8C) as a starting material, a rapid synthesis of nitrogen-doped graphene quantum dots (N-GQDs) was achieved by steaming the as-prepared ZIF-8C with an acid vapour. We found that the obtained N-GQD material could be used as a fluorescent probe for the detection of ferric ions with both excellent selectivity and a low detection limit.

It is expected that the facile strategy presented in this study can be extended to the synthesis of graphene quantum dots doped with other heteroatoms upon a proper selection of initial MOF crystals as raw materials. This work provides a low-cost and eco-friendly method for the preparation of the N-GQDs as a new application of the MOFs-based materials.

Acknowledgements

The authors acknowledge the financial support from the 'One Hundred Talents Project Foundation Program', the 'Cross-Cooperation Program for Creative Research Teams' and the 'Western Light Program' from Chinese Academy of Sciences, the National Natural Science Foundation of China (21203244, 21473247), the 'Young Creative Sci-Tech Talents Cultivation Project of Xinjiang Uyghur Autonomous Region (2013711012)' as well as the 'Xinjiang International Science and Technology Cooperation Project (20146003)'.

Notes and references

[a]*Laboratory of Environmental Sciences and Technology, Xinjiang Technical Institute of Physics and Chemistry; Key Laboratory ofFunctional Materials and Devices for Special Environments, Chinese Academy of Sciences, 40-1 Beijing Road, Urumqi, Xinjiang, 830011, China; Tel: +86-991-3677875; Fax: +86-991-3838957; E-mail:yuanqh@ms.xjb.ac.cn*

[b]*University of Chinese Academy of Sciences, No.19A Yuquan Road, Beijing, 100049, China*

Electronic Supplementary Information (ESI) available: The XRD pattern of as-synthesized ZIF-8 nanocrystals; Simulated XRD pattern of ZIF-8 from the published crystal structure data; N_2 adsorption-desorption isotherms of ZIF-8 andZIF-8C; SEM image of the sphere-like ZIF-8C powder obtained after the acid vapour cutting; Time-dependent photoluminescence spectrum of a N-GQDs solution under 330 nm excitation at 25 ℃ (Xe lamp, 150W). See DOI: 10.1039/b000000x/

1 Z. P. Zhang, J. Zhang, N. Chen and L. T. Qu, *Energy Environ. Sci.*, 2012, **5**, 8869.

2 X. M. Geng, L. Niu, Z. Y. Xing, R. S. Song, G. T. Liu, M. T. Sun, G. S. Cheng, H. J. Zhong, Z. H. Liu, Z. J. Zhang, L. F. Sun, H. X. Xu, L. Lu and L. W. Liu, *Adv. Mater.*, 2010, **22**, 638.

3 S. J. Zhuo, M. W. Shao and S. T. Lee, *Acs Nano*, 2012, **6**, 1059.

4 L. L. Li, K. P. Liu, G. H. Yang, C. M. Wang, J. R. Zhang and J. J. Zhu, *Adv. Funct. Mater.*, 2011, **21,** 869.

5 S. J. Zhu, J. H. Zhang, S. J. Tang, C. Y. Qiao, L. Wang, H. Y. Wang, X. Liu, B. Li, Y. F. Li, W. L. Yu, X. F. Wang, H. C. Sun and B. Yang, *Adv. Funct. Mater.*, 2012, **22**, 4732.

6 W. Li, Z. H. Zhang, B. A. Kong, S. S. Feng, J. X. Wang, L. Z. Wang, J. P. Yang, F. Zhang, P. Y. Wu and D. Y. Zhao, *Angew. Chem. Int. Ed.*, 2013, **52**, 8151.

7 Q. Q. Li, S. Zhang, L. M. Dai and L. S. Li, *J. Am. Chem. Soc.*, 2012, **134**, 18932.

8 Q. Liu, B. D. Guo, Z. Y. Rao, B. H. Zhang and J. R. Gong, *Nano lett.*, 2013, **13**, 2436.

9 D. L Jiang, Y. Zhang, H. Y. Chu, J. Liu, J. Wan and M. Chen, *Rsc Adv.*, 2014, **4**, 16163.

10 Y. Li, Y. Zhao, H. H. Cheng, Y. Hu, G. Q. Shi, L. M. Dai and L. T. Qu, *J. Am. Chem. Soc.*, 2012, **134**, 15.

11 M. Li, W. B. Wu, W. C. Ren, H. M. Cheng, N. J. Tang, W. Zhong and Y. W. Du, *Appl. Phys. Lett.*, 2012, **101,** 103107.

12 Z. S. Qian, J. Zhou, J. R. Chen, C. Wang, C. C. Chen and H. Feng, *J. Mater. Chem.*, 2011, **21**, 17635.

13 Y. Liu and P. Y. Wu, *ACS appl. Mater. Interfaces*, 2013, **5**, 3362.

14 L. B. Tang, R. B. Ji, X. M. Li, K. S. Teng and S. P. Lau, *J. Mater. Chem. C*, 2013, **1**, 4908.

15 H. Furukawa, K. E. Cordova, M. O'Keeffe and O. M. Yaghi, *Science.* 2013, **341**, 974; A. Morozan and F. Jaouen, *Energy Environ. Sci.*, 2012, **5**, 9269.

16 P. B. Gai, H. J. Zhang, Y. S. Zhang, W. Liu, G. B. Zhu, X. H. Zhang and J. H. Chen, *J. Mater. Chem. B*, 2013, **1**, 2742; X. J. Zhao, H. Y. Zhao, T. T. Zhang, X. C. Yan, Y. Yuan, H. M. Zhang, H. J. Zhao, D. M. Zhang, G. S. Zhu and X. D. Yao, *J. Mater. Chem. A*, 2014, **2**, 11666.

17 N. L. Torad, M. Hu, Y. Kamachi, K. Takai, M. Imura, M. Naito and Y. Yamauchi, *Chem. Commun.*, 2013, **49**, 2521.

18 M. Hu, J. Reboul, S. Furukawa, N. L. Torad, Q. M. Ji, P. Srinivasu, K. Ariga, S. Kitagawa and Y. Yamauchi, *J. Am. Chem. Soc.*, 2012, **134**, 2864.

19 J. Peng, W. Gao, B. K. Gupta, Z. Liu, R. Romero-Aburto, L. H. Ge, L. Song, L. B. Alemany, X. B. Zhan, G. H. Gao, S. A. Vithayathil, B. A. Kaipparettu, A. A. Marti, T. Hayashi, J. J. Zhu and P. M. Ajayan, *Nano lett.*, 2012, **12**, 844.

20 D. Y. Pan, J. C. Zhang, Z. Li and M. H. Wu, *Adv. Mater.*, 2010, **22**, 734.

21 L. L. Xiao, H. B. Xu, S. H. Zhou, T. Song, H. H. Wang, S. Z. Li, W. Gan and Q. H. Yuan, *Electrochim. Acta*, 2014, **143**, 143.

22 J. Ming, Y. Q. Wu, Y. C. Yu and F. Y. Zhao, *Chem. Commun.*, 2011, **47**, 5223.

23 Y. L. Zhang, L. Wang, H. C. Zhang, Y. Liu, H. Y. Wang, Z. H. Kang and S. T. Lee, *Rsc Adv.*, 2013, **3**, 3733.

24 Q. Liu, B. D. Guo, Z. Y. Rao, B. H. Zhang and J. R. Gong, *Nano Lett.*, 2013, **13**, 2436.

25 Y. Q. Dong, H. C. Pang, S. Y. Ren, C. Q. Chen, Y. W. Chi and T. Yu, *Carbon*, 2013, **64**, 245.

26 C. F. Hu, Y. L. Liu, Y. H. Yang, J. H. Cui, Z. R. Huang, Y. L. Wang, L. F. Yang, H. B. Wang, Y. Xiao and J. H. Rong, *J. Mater. Chem. B*, 2013, **1**, 39.

27 Y. Y. Shao, X. Q. Wang, M. Engelhard, C. M. Wang, S. Dai, J. Liu, Z. G. Yang and Y. H. Lin, *J. Power Sources*, 2010, **195**, 4375.

28 Y. Q. Dong, C. Q. Chen, X. T. Zheng, L. L. Gao, Z. M. Cui, H. B. Yang, C. X. Guo, Y. W. Chi and C. M. Li, *J. Mater. Chem.*, 2012, **22**, 8764.

29 L. B. Tang, R. B. Ji, X. K. Cao, J. Y. Lin, H. X. Jiang, X. M. Li, K. S. Teng, C. M. Luk, S. J. Zeng, J. H. Hao and S. P. Lau, *Acs Nano*, 2012, **6**, 5102.

30 M. Zhang, L. L. Bai, W. H. Shang, W. J. Xie, H. Ma, Y. Y. Fu, D. C. Fang, H. Sun, L. Z. Fan, M. Han, C. M. Liu and S. H. Yang, *J. Mater. Chem.*, 2012, **22**, 7461.

31 Z. S. Qian, C. Wang, G. H. Du, J. Zhou, C. C. Chen, J. J. Ma, J. R. Chen and H. Feng, *Crystengcomm*, 2012, **14,** 4976.

32 R. Z. Zhang and W. Chen, *Biosen. Bioelectron.*, 2014, **55**, 83.

33 R. L. Liu, D. Q. Wu, X. L. Feng and K. Mullen, *J. Am. Chem. Soc.*, 2011, **133**, 15221.

34 Y. M. Guo, Z. Wang, H. W. Shao and X. Y. Jiang, *Carbon*, 2013, **52**, 583.

35 D. Wang, L. Wang, X. Y. Dong, Z. Shi and J. Jin, *Carbon*, 2012, **50**, 2147.

36 S. K. Sahoo, D. Sharma, R. K. Bera, G. Crisponi, J. F. Callan, *Chem. Soc. Rev.*, 2012, **41**, 7195.

37 P. Li, Y. Zhao, L. Yao, H. R. Nie and M. Zhang, *Sens. Actuators B*, 2014, **191**, 332.

38 J. A. A. Ho, H. C. Chang and W. T. Su, *Anal. Chem.* 2012, **84**, 3246.

39 S. N. Qu, H. Chen, X. M. Zheng, J. S. Cao, X. Y. Liu, *Nanoscale*, 2013, **5**, 5514.

40 T. T. Lai, E. H. Zheng, L. X. Chen, X. Y. Wang, L. C. Kong, C. P. You, Y. M. Ruan and X. X. Weng, *Nanoscale*, 2013, **5**, 8015.

41 Y. Y. Du, M. Chen, Y. X. Zhang, F. Luo, C. Y. He, M. J. Li and X. Chen, *Talanta*, 2013, **106**, 261.

42 United States Environmental Protection Agency. National secondary drinking water regulations. Codes of Federal Register 40, Part 143, July 1, 2003. http://www.access.gpo.gov/nara/cfr/waisidx/waisidx 03/40cfr143 03. html

43 H. D. Huang, L. Liao, X. Xu, M. J. Zou, F. Liu and N. Li, *Talanta*, 2013, **117**, 152.

44 A. Ananthanarayanan, X. W. Wang, P. Routh, B. Sana, S. Lim, D. H. Kim, K. H. Lim, J. Li and P. Chen, *Adv. Funct. Mater.*, 2014, **24**, 3021.

45 J. Ju and W. Chen, *Biosens. Bioelectron.*, 2014, **58**, 219.

46 K. G. Qu, J. S. Wang, J. S. Ren and X. G. Qu, *Chem. Eur. J.*, 2013, **19**, 7243.

47 S. W. Zhang, J. X. Li, M. Y. Zeng, J. Z. Xu, X. K. Wang and W. P. Hu, *Nanoscale*, 2014, **6**, 4157.

48 Z. Chen, D. T. Lu, G. M. Zhang, J. Yang, C. Dong and S. M. Shuang, *Sens. Actuators B*, 2014, **202**, 631.

49 C. X. Yang, H. B. Ren and X. P. Yan, *Anal.Chem.*, 2013, **85**, 7441.

A new strategy for in-situ formation and separation of fluorescent N-GQDs for Fe^{3+} sensing was developed, with MOFs as precursors.